Macrofaunal burrowing Enhances Deep-sea Carbonate Lithification on the Southwest Indian Ridge

Hengchao Xu[1, 2], Xiaotong Peng[1]*, Shun Chen[1], Jiwei Li[1], Shamik Dasgupta[1], Kaiwen Ta[1], Mengran Du[1]

[1] Deep-sea Science Division, Institute of Deep-Sea Science and Engineering, Chinese Academy of Science, Sanya 572000, China

[2] Shcool of Ocean and Earth Science, Tongji University, Shanghai, 200092, China

Correspondence to: Xiaotong Peng (xtpeng@idsse.ac.cn)

Abstract. Deep-sea carbonates represent an important type of sedimentary rock due to their effect on the composition of the upper oceanic crust and their contribution to deep-sea geochemical cycles. However, the role of deep-sea macrofauna in carbonate lithification remains poorly understood. A large lithified carbonate area, characterized by thriving benthic faunas and a tremendous amount of burrows, was discovered in 2008, blanketing the seafloor of the ultraslow spreading Southwest Indian Ridge (SWIR). Benthic inhabitants, including echinoids, polychaetes, gastropods, and crustaceans, are abundant in this carbonate lithified area. The burrowing features within these carbonate rocks, and the factors that may influence deep-sea carbonate lithification, were examined. We suggest that burrowing in these carbonate rocks enhances deep-sea carbonate lithification. We propose that active bioturbation may trigger the dissolution of the original calcite and thus accelerate deep-sea carbonate lithification on mid-ocean ridges. Macrofaunal burrowing provides a novel driving force for deep-sea carbonate lithification at the seafloor, illuminating the geological and biological importance of bioturbation in global deep-sea carbonate rocks.

1 Introduction

Carbonate rocks and various types of sediments have been discovered on mid-ocean ridges through dredging or drilling (Thompson et al., 1968; De et al., 1985; Cooke et al., 2004). These carbonates, which are important elements of the upper oceanic crust, cover approximately half of the area of the entire ocean floor. As such, they may influence the composition of the oceanic crust and alter the geochemical balance between the total amounts of calcium, magnesium, and carbon in oceanic waters (Holligan and Robertson, 1996; Rae et al., 2011; Yu et al., 2014; Anderson et al., 1976).

Most carbonates in the deep sea are biogenic in origin and may include diagenetic products that originate from calcareous biogenic debris. The loss of porosity with increasing age and burial depth is associated with the transformation of deep-sea calcareous ooze to chalk and, subsequently, to limestone (Flügel, 2004). Nevertheless, the processes involved in the formation of deep-sea carbonate rocks remain controversial. It has commonly been assumed that deep-sea carbonate lithification is driven by various processes, including gravitational compaction, pressure dissolution, and reprecipitation, that

take place during burial (Croizé et al., 2013). The local dissolution and reprecipitation of biogenic calcite or aragonite from foraminifera, nanofossils, and pteropod oozes may serve to transform the original sediments to chalk or limestone (Schlanger and Douglas, 1974). These processes, however, cannot completely explain the observation that: (i) the degree of burial is commonly inconsistent with the known burial depth and paleontological age (Schmoker and Halley, 1982); and (ii) lithified carbonate rocks found on the seafloor commonly show no evidence of burial (Thompson et al., 1968). The lithification of deep-sea carbonates has also been associated with the breakdown of oceanic basalts or prolonged exposure to the chemical gradients at the sediment-water interface (Pimm et al., 1971; Bernoulli et al., 1978). However, the processes responsible for such seafloor lithification remain debated.

Benthic fauna burrowing into the substrate plays a critical role in sediment evolution, because they enhance the interactions between sediments, interstitial water and overlying water by changing the geochemical gradients in the sediment, restructuring bacterial communities, and influencing the physical characteristics of the sediments (Furukawa, 2001; Lohrer et al., 2004; Meysman et al., 2006; Barsanti et al., 2011; Lalonde et al., 2010 van de Velde and Meysman, 2016). Although burrowing has already been recognized as a factor that may influence $CaCO_3$ sediment profiles (Emerson and Bender, 1981; Aller, 1982; Emerson et al., 1985; Green et al., 1992) and may promote carbonate dissolution in coastal sediments (Gerino et al., 1998), little is known about the lithification effects on semi-lithified and lithified carbonate rocks in deep sea settings.

Nonburial carbonate samples were collected in 2008 near a newly discovered hydrothermal vent on the Southwest Indian Ridge (SWIR) during the DY115-20 cruise of R/V Dayang Yihao, which was conducted by the China Ocean Mineral Resource R&D Association (COMRA) (Fig. 1). These carbonate rocks, which were associated with thriving benthic biota, are characterized by numerous macrofaunal burrows. In this research, we examined this intriguing occurrence of nonburial carbonate lithification in the deep-sea and highlight the interactions that take place between bioturbation and lithification on the mid-ocean ridge.

2. Geological Setting

The Southwest Indian Ridge (SWIR), which is the major boundary between the Antarctic Plate and the African Plate, and is characterized by ultraslow and oblique expansion, is one of the slowest-spreading ridges (1.4-1.6 cm/yr) in the global ocean ridge system (Dick et al., 2003). Three main ridge sections of the eastern part of the SWIR are divided by the Gallieni Transform Fault (GTF) and the Melville Transform Fault (MTF) (Cannat et al., 1999). In 2008, a large lithified carbonate area, approximately 15 km long and 150 km wide, was found at water depths of 2000 to 2500 m on segment 26 of the SWIR, near a newly discovered hydrothermal field (Fig. 1). It has been widely reported that primary productivity increased substantially in the Indian Ocean during the Late Miocene–Early Pliocene (Arumugm et al., 2014; Gupta et al., 2004; Rai and Singh, 2001; Singh et al., 2012). This phenomenon known as the "biogenic bloom" promoted the deposition of high quantities of carbonate at the seafloor between 9 to 3.5 Ma (Gupta et al., 2004; Dickens and Owen, 1999).

3. Material and Methods

3.1 Sampling

The deep-sea carbonate samples were collected in 2008 by a TV-grab bucket operated from the R/V Da Yang Yi Hao. The survey sites covered an area that was approximately 15 km long and 150 km wide. When carbonate samples were spread on the deck, benthic organisms were usually evident among the fractured rocks. These organisms were identified in classes of echinoids, polychaetes, gastropods, and crustaceans in hand specimens. Samples were subsampled after recovery, and then stored at -20°C in plastic bags for mineralogical and geochemical analysis. Subsamples used for molecular phylogenetic analysis were kept frozen in dry ice and transported to the laboratory.

3.2 Computerized X-ray tomography (CT)

The quantitative measurement of the significance of biological influence is difficult because the physico-chemical properties around burrow walls are dynamic. Computerized X-ray tomography is a nondestructive method that has been used to measure various rock properties (e.g., bulk density, porosity, macropore size) by determining the numerical value of the X-ray attenuation coefficient. For relatively homogeneous marine sediments, this coefficient is expressed as Hounsfield units (HU), which is correlated with sample density (Michaud et al., 2003). In this study, computerized X-ray tomography measurements were performed using a GE Light Speed VCT instrument located in the Shanghai 10th People Hospital, Tongji University. CT images were computerized by reconstructng the distribution function of the linear attenuation coefficient, each with a 64-slice system with 64×0.625 mm detector banks and a z-axis coverage of 40 mm. The slice thickness was 2.5 mm, and the accuracy of distance measurements in the x and y-planes was 0.2 mm. The instrument operated at 140 kV, with a current of 10 mA, and an exposure of 1.5 s.

CT images were further characterized by *ImageJ*, which is a public domain Java-based image processing program. Gray values, which were correlated with the attenuation values and HU, were extracted to make a comparative description of the density changes of the carbonate sample. A total of 40 CT images were selected, and each gray value inverted using min = 0 and max = 255 regardless of the data values; that is, the theoretical integrated density value without the carbonate sample will be close to zero. The calibration function was used to calibrate whole images to a set of density standards before extracting. After all images selected were calibrated, the integrated density of the rock around the burrows could be calculated from the gray values. For this study, the gray values of the 10 pixels (approximately 0.3 cm, compared to the diameters of burrows, which are approximately 0.9 cm) around the burrow holes were measured. Additionally, randomly selected areas away from the burrows were selected as controls. The MATLAB function polyfit was used to interpret the difference between two data sets with 95% confidence bounds.

3. 3 X-ray diffraction (XRD)

Small pieces of the samples, which were freeze-dried under vacuum conditions to avoid oxidation during drying, were thoroughly ground using a pestle and mortar to produce a fine-grained, uniform powder. These powders were analysed using a D/max2550VB3+/PC X-ray diffractometer (Rigaku Corporation) at 40 kV and 30 mA, which is housed at the State Key Laboratory of Marine Geology at Tongji University.

3. 4 Scanning electron microscope (SEM)

Small fragments of the dried samples were fixed onto aluminum stubs with two-way adherent tabs, and allowed to dry overnight. They were sputter coated with gold for 2-3 minutes before being examined on a Philips XL-30 scanning electron microscope equipped with an accelerating voltage of 15kV at the State Key Laboratory of Marine Geology, Tongji University. The elemental composition of selected spots was determined by energy dispersive X-ray (EDX) analysis on the SEM with an accelerating voltage of 20 kV.

3.5 Element and isotope analysis

After the fusion of 0.1 g of sample material with 3.6 g of dilithium tetraborate at 1050 °C for ca. 16 min, major elements were measured using X-ray fluorescence Shimadzu XRF-1800 spectrometer at 40 kV and 95 mA that is located at Shanghai University. The trace element and rare earth element (REE) compositions of the samples were determined by inductively coupled plasma-mass spectrometry (ICP-MS) using a Thermo VG-X7 mass spectrometer at the State Key Laboratory of Marine Geology, Tongji University. Samples used for these analyses were dissolved using a solution of HNO_3 + HF on a hot plate. The eluted sample was then diluted with 2% HNO_3. The analytical precision and accuracy, monitored by the geostandard GSD9 and sample duplicates, were better than 5%.

The stable oxygen and carbon isotope ratios of bulk samples were measured using a Finnigan MAT252 isotope ratio mass spectrometer equipped with a Kiel III carbonate device at the State Key Laboratory of Marine Geology, Tongji University. Bulk samples were oven-dried at 60°C. Analytical precision was monitored using the Chinese national carbonate standard, GBW04405. The conversion of measurements to the Vienna Peedee Belemnite (PDB) scale was performed using NBS-19 and NBS-18.

4. Results

4.1 Macroscopic observations

The carbonate rocks retrieved from the SWIR were characterized by complex honeycombed structures, with Mn- and Fe-oxides commonly encrusting the surface and inner surface of the carbonate rocks (Fig. 2). Benthic inhabitants, including echinoids, polychaetes, gastropods, and crustaceans, which are usually recognized as successful burrowing classes in marine

sediments (Kristensen and Kostka, 2013), were abundant in hand specimens (Fig. 2c, d). the burrows drilled by benthic fauna revealed by CT scanning images are in straight, branched, or J- and U-shaped, with a density of up to 12 per dm^2 (Fig. S1). Burrows commonly penetrate 6 to 10 cm into the rock and are several millimeters to 2 cm in diameter. The area that surrounds the hole is usually brighter than that away from the burrow, which may indicate a different degree of lithification (Fig. 3a, 4a). Burrows can be classified in three categories. Burrows with living organisms can be categorized explicitly as fresh burrows (Fig. 2c, d). The second type is considered to be vacant burrows, which are filled by gray excrements (Fig. 2b). Thin black Mn- and Fe-oxide precipitates commonly encrust the surface of carbonate and the inner surface of empty burrows (Fig. 2a, c, d) and are thus classified as the third type of burrow. It has been suggested that Mn- and Fe-oxide precipitates grow at a very slow rate of 1-10mm/Ma. Coatings of black Mn- and Fe-oxide precipitates on the surface of the burrows indicate that they may have formed much earlier than the other burrows. Thus, the influence of bioturbation in this area was most likely a continuous process during early lithification and could play a significant role in both geological and biological processes.

4. 2 Enhanced lithification around burrows

Computerized X-ray tomography (CT) was used for the better characterization of local changes in the density of the carbonate rocks, which would reflect their degree of lithification. A darker colour in the tomographic cross-section image of the sample represents lower attenuation and thus lower density and higher porosity. The most apparent feature of the CT image is the localized enhancement of density around the burrow (Fig. 3, 4). The shapes of the area with higher density around the holes are triangular, quadrangular, hexagonal, round or irregular (Fig. 3b, c). The integrated density profiles extracted from the tomographic cross-section images make the contrast of density change around the burrow clearer (Fig. 3d). The 3D reconstruction of the sample by CT exhibits the density enhancement around the burrow, which is consistent with the brightness enhancement around the burrow, as shown in hand specimen (Fig. 4). The statistical analysis of the density data of 113 burrows (Fig. 5) provides robust evidence for density enhancement around the burrows, illuminating the significant influence of bioturbation in lithification. In addition, the results of CT also show that density is generally higher at the bottom than at the top of the carbonate rocks (Fig. 4c).

4. 3 Mineralogy

Based on XRD and elemental analyses, these rock samples consisted almost entirely of calcite and detectable quartz and halite, which are typical for deep-sea chalk defined as soft, pure, earthy, fine-textured, usually white to light gray or buff limestone of marine origin, consisting almost wholly (90-99%) of calcite, formed mainly by the accumulation of calcareous tests of floating microorganisms (chiefly foraminifers) and comminute remains of calcareous algae (such as coccoliths and rhabdoliths) set in a structureless matrix of very finely crystalline calcite (Wolfe, 1968; Flügel, 2004). Thin section and scanning electron photomicrographs show that biogenic components, mainly planktonic foraminifera (*Globigerina bulloides*) and cocolithophorid (*Coccolithus pelagicus*), are dominant (Fig. 6). The presence of *Globigerina bulloides* indicates that the

lithification history of carbonate rocks is less than 5 Ma (Pliocene-Recent) old. Therefore, the carbonate deposits on the SWIR could represent bioclastic deposition from the "biogenic bloom", which was the productivity related event in a large part of Indian Ocean during the middle Miocene to the early Pliocene (Singh et al., 2012; Rai and Singh, 2001; Gupta et al., 2004; Arumugm et al., 2014).

5   Although it was difficult to separate and quantify small tests from the very fine matrix, the carbonates exhibited a relatively high test to matrix ratio that is representative of deep-sea chalk (Fig. 6a). Original skeletal grains were held together by cement. Body chambers in the foraminiferal tests, for instance, were partially filled by calcite cements (Fig. 6b, c). It was common to observe the accretionary overgrowth of calcite around the foraminifera test from SEM images (Fig. 6c). The dissolution of the coccolith plates is evident both on the surface of the thin black Mn- and Fe-oxide precipitates and in

10   the interior of carbonate rocks (Fig. 6d, e). The gray excrements filling in the burrow primarily consisted of plates of coccolithophorids (*Calcidiscus leptoporus, Emiliania huxleyi* and *Gephurocapsa oceanica*). The smooth surfaces of the coccoliths in gray excrements revealed that dissolution commonly occurs influenced by the bioleaching of benthic fauna (Fig. 6f).

4.4 Geochemistry and isotope analysis

15   Three types of samples (chalk, gray excrements and thin black Mn- and Fe-oxide precipitates) exhibited similar elemental concentration patterns with a high CaO content, reflecting the strong dilution effect of biogenic calcium (Table S1). One of the main characteristics of major and rare elements is the highly variable Sr concentration in different types of samples. The storage of Sr on the seafloor is mainly caused by its substitution for Ca in calcium carbonate, while diagenetic recrystallization results in the decrease of Sr from the sediment (Plank and Langmuir, 1998; Qing and Veizer, 1994). The

20   lower Sr/Ca ratio in chalk compared to those in the gray excrements could also be a response to the lithification of carbonate (Fig. 7). Although biogenic calcium diluted the detrital REE fraction, it made little direct contribution to the bulk REE concentrations (Xiong et al., 2012). The REE patterns in the three types of samples did not exhibit any hydrothermal anomalies, e.g., positive Eu anomalies, but they inherit the characteristics of sea water, exhibiting the enrichment of HREE over LREE and a negative Ce anomaly (except the Mn- and Fe-oxides) (Fig. 8). The influence of nearby hydrothermal

25   systems and detrital input to the studied carbonate area was negligible during the lithification history.

       The $\delta^{13}C_{PDB}$ values of 46 bulk samples ranged from -0.37 to 1.86‰, which are typical values for biogenic carbonates (e.g., Cook and Egbert 1979). These samples have a relatively narrow $\delta^{18}O_{PDB}$ range of 1.35 to 3.79‰. The positive correlation of $\delta^{13}C_{PDB}$ and $\delta^{18}O_{PDB}$ values in chalk and gray excrements (r = 0.91) reveals the minor environmental influence on early lithification (Fig. 9), and bioturbation should be a critical factor during the lithification. There is an evident

30   depletion of carbon and oxygen isotopic values in gray excrements compared to those in chalks (Fig. 9). The carbon isotope signatures of carbonates near burrows were higher than those in undisturbed areas (Table 1).

5. Discussion

5.1 Bioturbation in carbonate rock on the SWIR

The dimensions of burrows can be estimated from tomographic cross-section of the samples. Burrows were generally a few millimeters to 2 cm in diameter, commonly penetrating 6 to 10 cm into the rocks and ultimately reaching a density of up to 12 per dm^2. If the burrows in straight, branched, or J and U shapes (Fig. 2e) are simplified to a cylinder with the diameter of 1 cm and height of 6 cm, which are the median values of the burrows, then the estimated volume of the simplified cylinder can be used to determine the extent of substratum reconstruction by bioturbation. In this model, a 1 dm^2 surface area which can harbor 12 burrows on the surface, may reach up to 0.226 dm^3 of burrow space. Eventually, we can deduce that the carbonate substratum has been reconstructed by bioturbation to a great extent.

Benthic fauna maintain burrows for certain purposes, such as gaseous exchange, food transport, gamete transport, transport of environmental stimuli, and removal of metabolites (Kristensen and Kostka, 2013). Polychaetes, the most successful burrow class for example (Díaz-Castañeda and Reish, 2009), were abundant, and they conventionally produced J- or U- shaped burrows that extended as long as several decimeters in hand specimens (Fig. 2 c, e). Relic burrows allow sea water to directly penetrate into the carbonate rocks, which is beneficial for the precipitation of black Mn- and Fe-oxide precipitates on the inner surface of the burrow (Fig. 2a, c). The genetic models for Mn- and Fe-oxide precipitates attribute the precipitation of minerals out of the cold ambient seawater onto the rock surface to the aid of biogenic activity (Hein and Koschinsky, 2014). Burrowing benthic fauna excrete mucus to garden their burrow holes by incorporating organic matter into the walls (Dworschak et al., 2006; Koller et al., 2006; Petrash et al., 2011). The mucus layer may act as a favorable site for the accumulation of metallic ions through organo-metallic complexation or chelation at suitable Eh, pH and redox conditions (Lalonde et al., 2010; Banerjee, 2000). Thus, along with carbonate reworking and biomixing during the frequent construction and maintenance of a burrow, mineralogical and geochemical parameters are also assumed to oscillate around the burrow.

In addition to burrowing activity, benthic fauna ingest and excrete the substrate which usually serves the burrows as traps for fecal pellets (Fig. 2b) (Hydes, 1982; Aller and Aller, 1986). Although benthic fauna ingest organically enriched particles, thus removing the organic matter, bulk samples are often still enriched in residual fecal material (Dauwe et al., 1998). Regardless, organic matter influenced by bioturbation and delivered as biodeposits in surface sediments, and vice versa, may therefore create a dynamic and heterogeneous chemical, physical, and biological microenvironment in deep-sea carbonate zones. Eventually, a microenvironment friendly for heterotrophic microorganisms may formed in the carbonate due to the redistribution of organic particles. The biodiversity of the prokaryotic communities within the samples examined by Li et al. (2014) indicated that the distribution of Acidobacteria and Bacteroidetes noted in this study might indicate the greater organic carbon availability in the interior carbonates. Alternatively, bacterial metabolites and organic detritus are considered to be the major sources of food for benthic fauna in deep-sea environments, which are limited by the availability

of organic matter (Raghukumar et al., 2001). Thus, a balanced ecological sustainability is established by carbonate deposits and continuous biological processes, which may largely influence the lithification history of carbonates.

5. 2 Roles of bioturbation in lithification of carbonate rocks on the SWIR

The abundant macrofaunal burrows and benthic fauna (e.g., polychaete worm, Fig. 2c) present on a cross section of carbonate rocks, as well as enhanced density around burrows commonly observed from CT images (Fig. 3, 4), provided robust evidence for the significant role of bioturbation in present lithified deep-sea carbonates. The lithification of carbonate is confirmed by the dissolution of coccolith plates observed by SEM (Fig. 6) and the change in elemental composition between different portions of the carbonate (Fig. 7). The water depth of the studied carbonate area on the SWIR varies approximately from 2000 to 2500 meters (Fig. 1), which is above the calcite saturation horizon (Broecker et al., 1982). In this range of water depth, the key point of carbonate lithification is how original tests or plates are dissolved under saturation conditions. Although less stable $CaCO_3$ phases (e.g., biogenic, high-Mg calcites) may dissolve above the calcite saturation horizon (Jahnke and Jahnke, 2004), that is not likely to occur here since our samples are low-Mg calcites. As a general rule, compaction takes place with the gradual increase in overburden pressure, resulting in the loss of porosity through mechanical and chemical compaction in the moderatelt deep burial stage. However, the carbonate samples studied here have never been buried. Their lithification, therefore, may be different from those of other deep sea carbonates. We deduced from elemental and isotopic results that the influence of nearby hydrothermal systems and other detrital input to the studied carbonate area should be negligible during the lithification history. The construction and ventilation of burrows can fundamentally alter biogeochemical processes and produce lateral heterogeneity, thus intensifying the redistribution of pore water fluids. Moreover, ecological niches for microbial life are also formed by bioturbation (Ghirardelli, 2002; Koretsky et al., 2013). Thus, the simultaneous activity of both thriving benthic fauna and the lithification of carbonate are potentially connected.

The organic matter content is significantly low in the deep-sea sediments. However, the distribution and diversity of the prokaryotic communities inhabiting carbonate samples imply greater organic carbon availability in the interior carbonates compared to the exterior (Li et al., 2014). It is known that polychaetes' mixing sediment particles is an important driving force behind the chemical reaction and transport of organic matter in marine sediments (Berner and Westrich, 1985). Benthic fauna, including polychaetes, reconstruct the carbonate substratum to a great extent, which results in the fundamental alteration of their sedimentary environment. The aerobic respiration of bioturbated organic particles, such as mucus, would positively contribute to the aerobic respiration of bioturbated organic particles by heterotrophic (micro)organisms (Lohrer et al., 2004), whose reaction product, CO_2, may be responsible for lowering the pH of porewater around the burrow relative to the inner carbonate sediment, which may drive the dissolution of original calcite in the microenvironment (Fig. 10) (Emerson and Bender, 1981; Aller, 1982; Kristensen, 2000). The isotopic composition in gray excrements is lighter when compared to the chalks (Fig. 9; Table 1). It is assumed that fecalpellets may be strongly depleted in ^{13}C in isotopic mass balance with the ^{13}C enrichment of the organism (Damste et al., 2002). That means bioturbated organic particles, such as mucus, will inherit enriched ^{13}C, which is the major carbon source for microbial metabolic reaction. The local elevated

concentration of dissolved CO_2 in pore water would trigger the dissolution of the original $CaCO_3$ phases, which is consistent with the results of SEM observations. For instance, the body chambers in the foraminiferal tests are partially filled by calcite cements (Fig. 6c), which is believed to be derived internally through solution transfer (Durney, 1972).

In addition, relic burrows allow sea water to directly penetrate into carbonate rocks and lead to the precipitation of black Mn- and Fe-oxide precipitates in the inner surface of the burrow. The microbial oxidation of Fe^{2+} and Mn^{2+} in these sites would also greatly accelerate the dissolution of $CaCO_3$ fossils (Emerson and Bender, 1981; Aller and Rude, 1988). Furthermore, thin Mn- and Fe-oxide precipitates may preventrapid ion exchange between bottom water and porewater within carbonate rocks. Ca^{2+} and CO_3^{2-}, the products of $CaCO_3$ dissolution, prefer to diffuse to the interior of carbonate rocks, and lead to the reprecipitation of calcites as cements with higher$\delta^{13}C_{PDB}$ values in carbonate rocks (Fig. 10).

6. Conclusions

A lithified carbonate area characterized by active bioturbation was studied to explore the biological and geological interactions in this area. Although different parameters influenced by bioturbation cannot be easily differentiated in a study of natural samples, available evidence shows that active bioturbations may trigger the dissolution of original calcite above the saturation horizon, thus enhancing the deep-sea carbonate lithification on mid-ocean ridges. The novel mechanism proposed here for nonburial carbonate lithification at the deep-sea seafloor sheds light on the potential interactions between deep-sea biota and sedimentary rocks and also illuminates the geological and biological importance of bioturbation on global deep-sea carbonate rocks.

Author contributions: This work was designed by XP and performed by HX, SC, KT, SD, JL, and MD. JL collected the samples. HX and XP led the writing of the papers and prepared the figures with contributions from all co-authors.

Acknowledgments

Special thanks go to all the participants of the cruise of R/V DayangYihao conducted by the China Ocean Mineral Resource R&D Association (COMRA) in 2008. The authors also would like to acknowledge Dr. Sui Wan at Tongji University for his help with calcareous fossil analysis. Financial support for this research came from the "National key research and development plan of China" (2016YFC0304900), the "Strategic Priority Research Program" of the Chinese Academy of Science (Grant No. XDB06020000), the "National Key Basic Research Program of China" (2015CB755905), and the "Natural Science Foundation of Hainan Province, China" (20164175). We are indebted to Prof. Brian Jones at the University of Alberta for his valuable suggestions on the manuscript. We are greatly indebted to two anonymous journal reviewers and the journal associate editor, Caroline Slomp, for their critical comments on an earlier version of this manuscript.

References

Aller, J. Y., and Aller, R. C.: Evidence for localized enhancement of biological associated with tube and burrow structures in deep-sea sediments at the HEEBLE site, western North Atlantic, DeepSea Res. Pt1, 33, 755-790, https://doi.org/10.1016/0198-0149(86)90088-9, 1986.

5   Aller, R. C.: Carbonate dissolution in nearshore terrigenous muds: the role of physical and biological reworking, The Journal of Geology, 90, 79-95, 1982.

Aller, R. C., and Rude, P. D.: Complete oxidation of solid phase sulfides by manganese and bacteria in anoxic marine sediments, Geochim. Cosmochim. Acta, 52, 751-765, https://doi.org/10.1016/0016-7037(88)90335-3, 1988.

Anderson, T., Donnelly, T., Drever, J., Eslinger, E., Gieskes, J., Kastner, M., Lawrence, J., and Perry, E.: Geochemistry and

10   diagenesis of deep-sea sediments from Leg 35 of the Deep Sea Drilling Project, Nature, 261, 473-476, https://doi.org/10.1038/261473a0, 1976.

Arumugm, Y., Gupta, A. K., and Panigrahi, M. K.: Species diversity variations in Neogene deep-sea benthic foraminifera at ODP Hole 730A, western Arabian Sea, J. Earth Syst. Sci., 123, 1671-1680, https://doi.org/10.1007/s12040-014-0495-z, 2014.

Banerjee: A documentation on burrows in hard substrates of ferromanganese crusts and associated soft sediments from the

15   Central Indian Ocean, Curr. Sci. India., 79, 517-521, 2000.

Barsanti, M., Delbono, I., Schirone, A., Langone, L., Miserocchi, S., Salvi, S., and Delfanti, R.: Sediment reworking rates in deep sediments of the Mediterranean Sea, Sci. Total. Environ., 409, 2959-2970, http://doi.org/10.1016/j.scitotenv.2011.04.025, 2011.

Berner, R. A., and Westrich, J. T.: Bioturbation and the early diagenesis of carbon and sulfur, Am. J. Sci., 285, 193-206,

20   http://doi.org/10.2475/ajs.285.3.193, 1985.

Bernoulli, D., Garrison, R., and McKenzie, J.: Petrology, isotope geochemistry, and origin of dolomite and limestone associated with basaltic breccia, Hole 373A, Tyrrhenian Basin, in: Initial Reports of the Deep Sea Drilling Projec, edited by: KJ Hsü, and Montadert, L., 1, U. S. Government Printing Office, Washington 541-558, 1978.

Broecker, W. S., Peng, T.-H., and Beng, Z.: Tracers in the Sea, Lamont-Doherty Geological Observatory, Columbia

25   University, New York, 1982.

Cannat, M., Rommevaux-Jestin, C., Sauter, D., Deplus, C., and Mendel, V.: Formation of the axial relief at the very slow spreading Southwest Indian Ridge (49 to 69 E), J. Geophys. Res.-Sol. Ea. (1978–2012), 104, 2825-2843, https://doi.org/10.1029/1999JB900195, 1999.

Cook H. E., Egbert R.M.: Diagenesis of Deep-Sea Carbonates. in: Larsen G, Chilingar GV, eds. Developments in

30   Sedimentology, Elsevier. 213-288, 1979.

Cooke, P. J., Nelson, C. S., Crundwell, M. P., Field, B., Elkington, E. S., and Stone, H.: Textural variations in Neogene pelagic carbonate ooze at DSDP Site 593, southern Tasman Sea, and their paleoceanographic implications, New Zeal. J. Geol. Geop., 47, 787-807, https://doi.org/10.1080/00288306.2004.9515089, 2004.

Croizé, D., Renard, F., and Gratier, J.-P.: Compaction and porosity reduction in carbonates: a review of observations, theory, and experiments, Adv. Geophys., 54, 181-238, http://doi.org/10.1016/B978-0-12-380940-7.00003-2, 2013.

Díaz-Castañeda, V., and Reish, D. J.: Polychaetes in Environmental Studies, in: Annelids in Modern Biology, John Wiley & Sons, Inc., 203-227, 2009.

5   Damste, J. S. S., Breteler, W. C. M. K., Grice, K., Van Rooy, J., and Schmid, M.: Stable carbon isotope fractionation in the marine copepod Temora longicornis : Unexpectedly low δ^{13}C value of faecal pellets, Mar. Ecol–Prog. Ser., 240, 195-204, https://doi.org/10.3354/meps240195, 2002.

Dauwe, B., Herman, P. M. J., and Heip, C. H. R.: Community structure and bioturbation potential of macrofauna at four North Sea stations with contrasting food supply, Mar. Ecol–Prog. Ser., 173, 67-83, https://doi.org/10.3354/meps173067, 10   1998.

De, R., Rao, C. N., and Kaul, I. K.: Implications of diagenesis for the TL dating of the oceanic carbonate sediments in the Northern Indian ocean, Nucl. Tracks. Radiat. Meas., 10, 185-192, 1985.

Dick, H. J., Lin, J., and Schouten, H.: An ultraslow-spreading class of ocean ridge, Nature, 426, 405-412, https://doi.org/10.1038/nature02128, 2003.

15   Dickens, G. R., and Owen, R. M.: The Latest Miocene–Early Pliocene biogenic bloom: a revised Indian Ocean perspective, Mar. Geol., 161, 75-91, http://doi.org/10.1016/S0025-3227(99)00057-2, 1999.

Dworschak, P. C., Koller, H., and Abed-Navandi, D.: Burrow structure, burrowing and feeding behaviour of Corallianassa longiventris and Pestarella tyrrhena (Crustacea, Thalassinidea, Callianassidae), Mar. Biol., 148, 1369-1382, https://doi.org/10.1007/s00227-005-0161-8, 2006.

20   Emerson, S., and Bender, M.: Carbon fluxes at the sediment-water interface of the deep-sea: calcium carbonate preservation, J. Mar. Res., 39, 139-162, 1981.

Emerson, S., Fischer, K., Reimers, C., and Heggie, D.: Organic carbon dynamics and preservation in deep-sea sediments, Deep-sea Res. PT1., 32, 1-21, 1985.

Flügel, E.: Diagenesis, Porosity, and Dolomitization, in: Microfacies of Carbonate Rocks: Analysis, Interpretation and 25   Application, Springer Berlin Heidelberg, 267-338, https://doi.org/10.1007/978-3-662-08726-8_7, 2004,.

Furukawa, Y.: Biogeochemical consequences of macrofauna burrow ventilation, Geochem. T., 2, 1-9, https://doi.org/10.1186/1467-4866-2-83, 2001.

Gerino, M., Aller, R. C., Lee, C., Cochran, J. K., Aller, J. Y., Green, M. A., and Hirschberg, D.: Comparison of different tracers and methods used to quantify bioturbation during a spring bloom: 234-Thorium, Luminophores and Chlorophylla, 30   Estuar. Coast. Shelf S., 46, 531-547, http://doi.org/10.1006/ecss.1997.0298, 1998.

Ghirardelli: Endolithic Microorganisms in Live and Dead Thalli of Coralline Red Algae (Corallinales, Rhodophyta) in the Northern Adriatic Sea, Acta geológica hispánica, 37, 53-60, 2002.

Green, M. A., Aller, R. C., and Aller, J. Y.: Experimental evaluation of the influences of biogenic reworking on carbonate preservation in nearshore sediments, Mar. Geol., 107, 175-181, https://doi.org/10.1016/0025-3227(92)90166-F, 1992.

Gupta, A. K., Singh, R. K., Joseph, S., and Thomas, E.: Indian Ocean high-productivity event (10–8 Ma): Linked to global cooling or to the initiation of the Indian monsoons?, Geology, 32, 753-756, https://doi.org/10.1130/g20662.1, 2004.

Hein, J. R., and Koschinsky, A.: Deep-Ocean Ferromanganese Crusts and Nodules A2 - Holland, Heinrich D, in: Treatise on Geochemistry (Second Edition), edited by: Turekian, K. K., Elsevier, Oxford, 273-291, 2014.

5   Holligan, P. M., and Robertson, J. E.: Significance of ocean carbonate budgets for the global carbon cycle, Global Change Biol., 2, 85-95, https://doi.org/10.1111/j.1365-2486.1996.tb00053.x, 1996.

Hydes, D. J.: Animal burrows in deep-sea sediments, 1982.

Jahnke, R. A., and Jahnke, D. B.: Calcium carbonate dissolution in deep sea sediments: Reconciling microelectrode, pore water and benthic flux chamber results, Geochim. Cosmochim. Ac., 68, 47-59, https://doi.org/10.1016/S0016-

10   7037(03)00260-6, 2004.

Koller, H., Dworschak, P. C., and Abed-Navandi, D.: Burrows of Pestarella tyrrhena (Decapoda: Thalassinidea): hot spots for Nematoda, Foraminifera and bacterial densities, J. Mar. Biol. Assoc. UK., 86, 1113-1122, https://doi.org/doi:10.1017/S0025315406014093, 2006.

Koretsky, C. M., Meile, C., and Van Cappellen, P.: Incorporating Ecological and Biogeochemical Information into Irrigation

15   Models, in: Interactions Between Macro- and Microorganisms in Marine Sediments, American Geophysical Union, 341-350, https://doi.org/10.1029/CE060p0341, 2013.

Kristensen, E.: Organic matter diagenesis at the oxic/anoxic interface in coastal marine sediments, with emphasis on the role of burrowing animals, Hydrobiologia, 426, 1-24, https://doi.org/10.1023/a:1003980226194, 2000.

Kristensen, E., and Kostka, J. E.: Macrofaunal Burrows and Irrigation in Marine Sediment: Microbiological and

20   Biogeochemical Interactions, in: Interactions Between Macro- and Microorganisms in Marine Sediments, American Geophysical Union, 125-157, https://doi.org/10.1029/CE060p0125, 2013.

Lalonde, S. V., Dafoe, L. T., Pemberton, S. G., Gingras, M. K., and Konhauser, K. O.: Investigating the geochemical impact of burrowing animals: Proton and cadmium adsorption onto the mucus lining of Terebellid polychaete worms, Chem. Geol., 271, 44-51, https://doi.org/10.1016/j.chemgeo.2009.12.010, 2010.

25   Li, J., Peng, X., Zhou, H., Li, J., Sun, Z., and Chen, S.: Microbial Communities in Semi-consolidated Carbonate Sediments of the Southwest Indian Ridge, J. Microbiol., 52, 111-119, https://doi.org/10.1007/s12275-014-3133-1, 2014.

Lohrer, A. M., Thrush, S. F., and Gibbs, M. M.: Bioturbators enhance ecosystem function through complex biogeochemical interactions, Nature, 431, 1092-1095, https://doi.org/10.1038/nature03042, 2004.

Meysman, F. J., Middelburg, J. J., and Heip, C. H.: Bioturbation: a fresh look at Darwin's last idea, Trends. Ecol. Evol., 21,

30   688-695, https://doi.org/10.1016/j.tree.2006.08.002, 2006.

Michaud, E., Desrosiers, G., Long, B., De Montety, L., Crémer, J.-F., Pelletier, E., Locat, J., Gilbert, F., and Stora, G.: Use of axial tomography to follow temporal changes of benthic communities in an unstable sedimentary environment (Baie des Ha! Ha!, Saguenay Fjord), J. Exp. Mar. Biol. Ecol., 285, 265-282, https://doi.org/10.1016/S0022-0981(02)00532-4, 2003.

Petrash, D. A., Lalonde, S. V., Gingras, M. K., and Konhauser, K. O.: A Surrogate approach to studying the chemical reactivity of burrow mucous linings in marine sediments, Palaios, 26, 594-600, https://doi.org/10.2110/palo.2010.p10-140r, 2011.

Pimm, A., Garrison, R., and Boyce, R.: Sedimentology synthesis: lithology, chemistry and physical properties of sediments in the northwestern Pacific Ocean, in: Initial Reports of the Deep Sea Drilling Projec, edited by: Fischer, A., and Heezen, B., U.S. Government Printing Office, Washington, 1131-1252, 1971.

Plank, T., and Langmuir, C. H.: The chemical composition of subducting sediment and its consequences for the crust and mantle, Chem. Geol., 145, 325-394, https://doi.org/10.1016/S0009-2541(97)00150-2, 1998.

Qing, H., and Veizer, J.: Oxygen and carbon isotopic composition of Ordovician brachiopods: Implications for coeval seawater, Geochim. Cosmochim. Ac., 58, 4429-4442, https://doi.org/10.1016/0016-7037(94)90345-X, 1994.

Rae, J. W. B., Foster, G. L., Schmidt, D. N., and Elliott, T.: Boron isotopes and B/Ca in benthic foraminifera: proxies for the deep ocean carbonate system, Earth Planet. Sc. Lett., 302, 403-413, https://doi.org/10.1016/j.epsl.2010.12.034, 2011.

Raghukumar, C., Bharathi, P. A. L., Ansari, Z. A., Nair, S., Ingole, B. S., Sheelu, G., Mohandass, C., Nath, B. N., and Rodrigues, N.: Bacterial standing stock, meiofauna and sediment-nutrient characteristics: Indicators of benthic disturbance in the Central Indian Basin, Deep-sea Res. PT2, 48, 3381-3399, https://doi.org/10.1016/S0967-0645(01)00047-9, 2001.

Rai, A. K., and Singh, V. B.: Late Neogene deep-sea benthic foraminifera at ODP Site 762B, eastern Indian Ocean: diversity trends and palaeoceanography, Palaeogeogr. Palaeocl.,, 173, 1-8, https://doi.org/10.1016/S0031-0182(01)00299-1, 2001.

Schlanger, S. O., and Douglas, R. G.: The Pelagic Ooze-Chalk-Limestone Transition and its Implications for Marine Stratigraphy, in: Pelagic Sediments: On Land and under the Sea, Blackwell Publishing Ltd., 117-148, 1974.

Schmoker, J. W., and Halley, R. B.: Carbonate porosity versus depth: a predictable relation for South Florida, AAPG Bulletin, 66, 2561-2570, 1982.

Singh, R. K., Gupta, A. K., and Das, M.: Paleoceanographic significance of deep-sea benthic foraminiferal species diversity at southeastern Indian Ocean Hole 752A during the Neogene, Palaeogeogr. Palaeocl., 361–362, 94-103, https://doi.org/10.1016/j.palaeo.2012.08.008, 2012.

Thompson, G., Bowen, V., Melson, W., and Cifelli, R.: Lithified carbonates from the deep-sea of the equatorial Atlantic, J Sediment. Res., 38, 1305-1312, 1968.

Van de Velde, S., and Meysman, F. J. R.: The influence of bioturbation on iron and sulphur cycling in marine sediments: a model analysis, Aquat. Geochem., 22, 469-504, https://doi.org/10.1007/s10498-016-9301-7, 2016.

Wolfe, M. J.: Lithification of a carbonate mud: Senonian chalk in Northern Ireland, Sediment. Geol., 2, 263-290, 1968.

Xiong, Zhifang, Li, Tiegang, Algeo, Thomas, Chang, Fengming, Yin, and Xuebo: Rare earth element geochemistry of laminated diatom mats from tropical West Pacific: Evidence for more reducing bottomwaters and higher primary productivity during the Last Glacial Maximum, Chem. Geol., 296–297, 103-118, https://doi.org/10.1016/j.chemgeo.2011.12.012, 2012.

Yu, J., Anderson, R. F., and Rohling, E. J.: Deep ocean carbonate chemistry and glacial-interglacial atmospheric CO_2 changes, Oceanography, 27, 16-25, 2014.

Zhu, J., Lin, J., Chen, Y. J., Tao, C., German, C. R., Yoerger, D. R., and Tivey, M. A.: A reduced crustal magnetization zone near the first observed active hydrothermal vent field on the Southwest Indian Ridge, Geophys. Res. Lett., 37, https://doi.org/10.1029/2010GL043542, 2010.
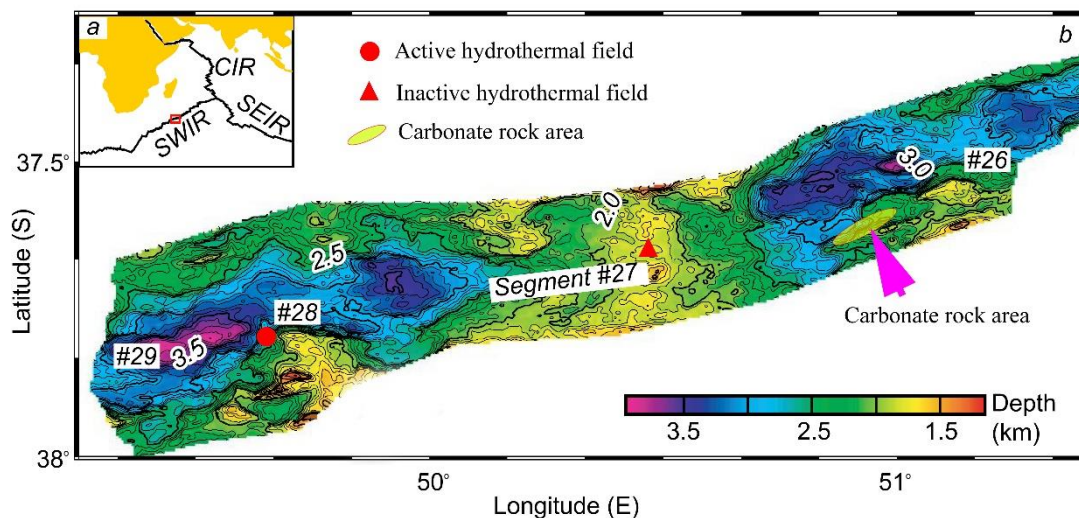
.

Figure 1: (a) Location of study area on the Southwest Indian Ridge (After Zhu et al., 2010). (b) Bathymetric map of area which show the location of the carbonate rock area (green ellipse), the active hydrothermal field (red cycle), and the inactive hydrothermal field (red triangle).
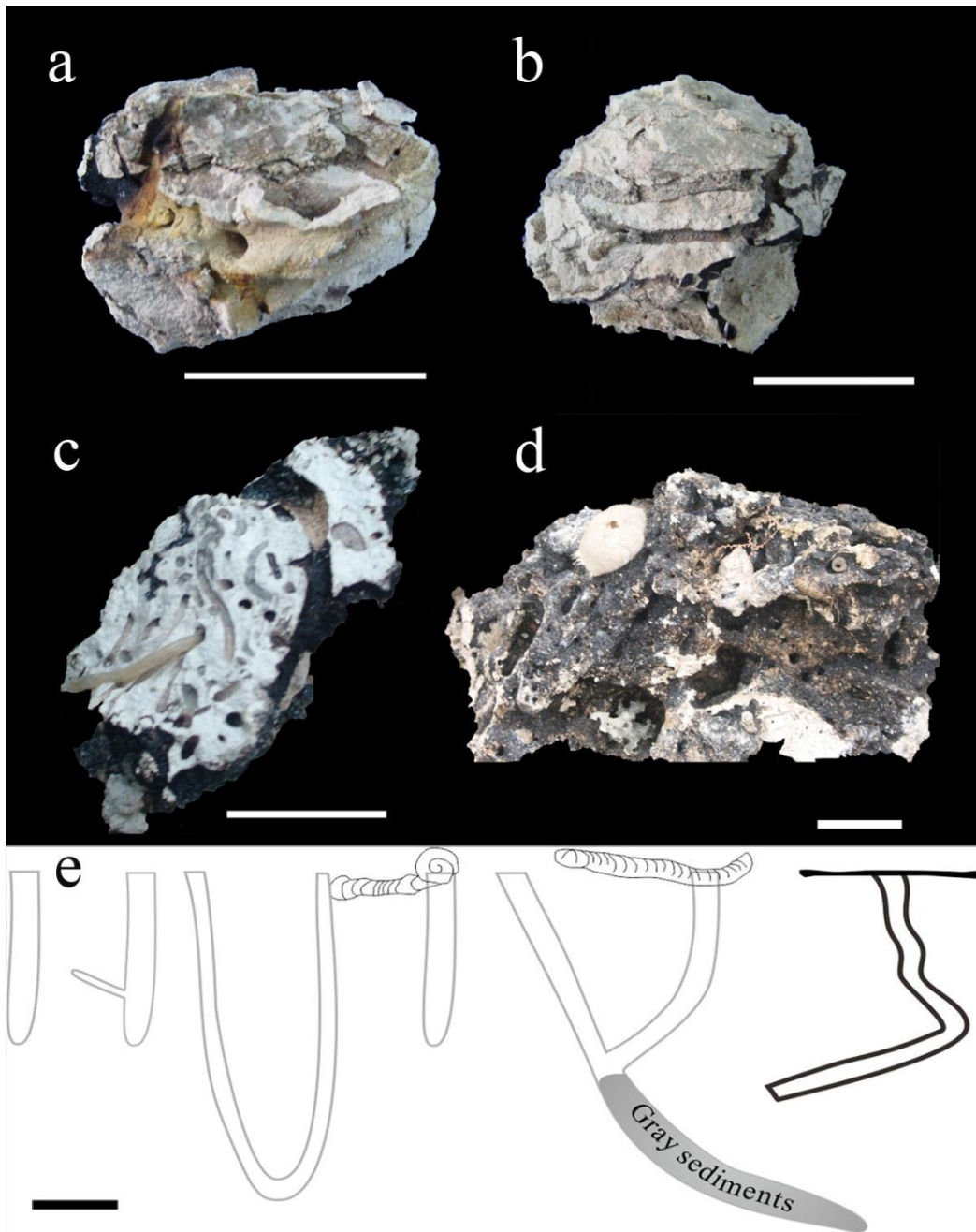
Figure 2: Deep-sea carbonate rocks collected from the SWIR. (a) A carbonate rock sample shows empty burrows are partly covered by ferromanganese crusts. (b) Straight and branched burrows are infilled by gray sediments. (c) Abundant burrows, as well as a benthic fauna (polychaete worm), are present on a cross section of a carbonate rock. (d) An echinoid, together with other benthic faunas, burrows in a carbonate rock with honeycomb structures and encrusted by thin ferromanganese crusts. (e) Sketch for different burrow structures in deep-sea carbonate rocks collected from the SWIR. Scale bar of a, c is 5 cm, and the b, d e is 3 cm.
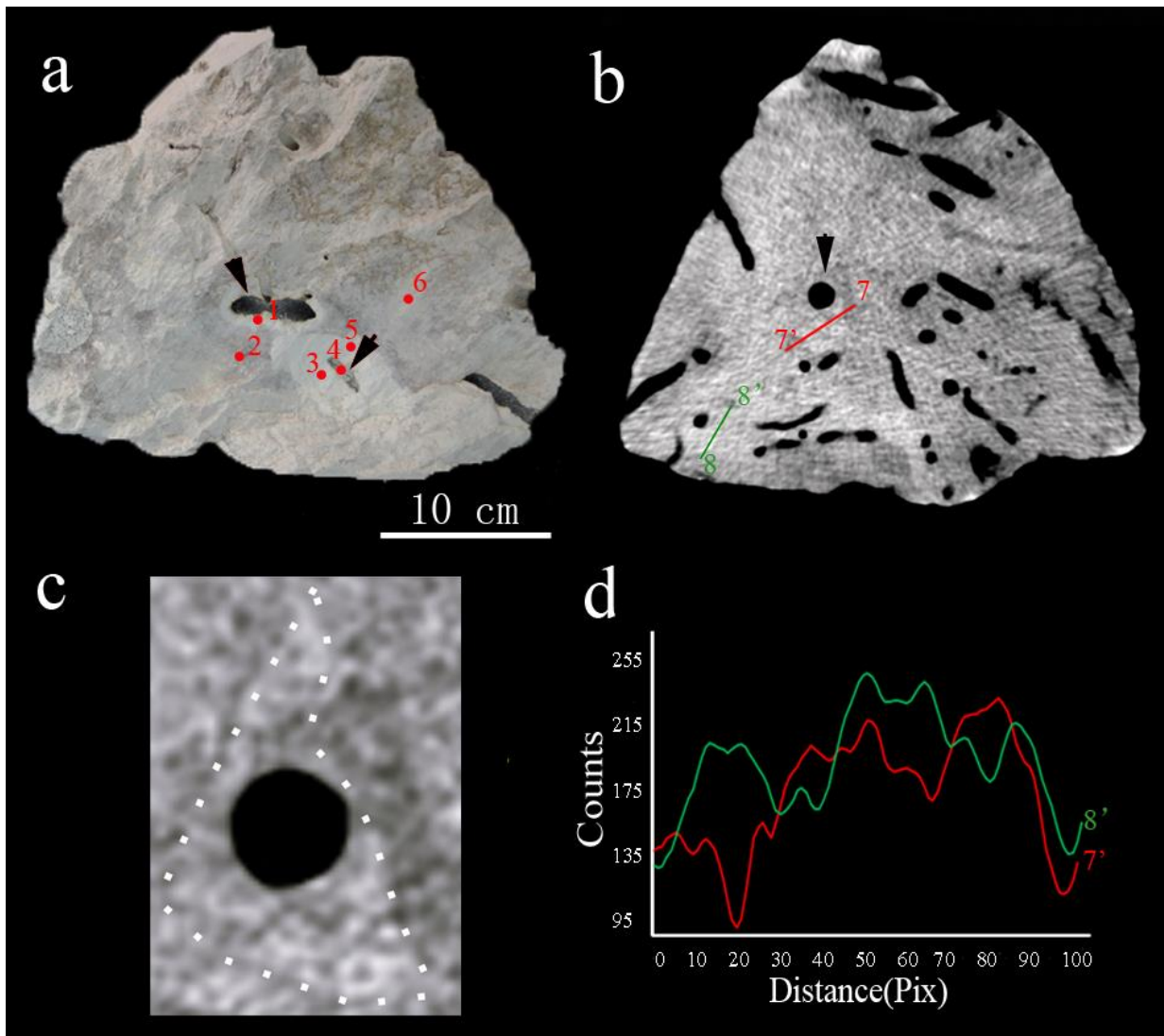
Figure 3: (a) A hand specimen shows the enhanced brightness associated with burrow structures. Numbers of red dots indicate the subsamples for carbon and oxygen isotopic analysis in Table 1. (b) Tomographic cross-section of the sample reveals that abundant burrows are clearly present in the interior of the samples. High density areas with triangular, hexagonal and irregular shapes. (c) The enlargement of Figure 3b shows the triangular shape with high density (white dash line). (d) Line scan profiles of gray values along solid line (7-7' and 8-8') in Figure 3b.
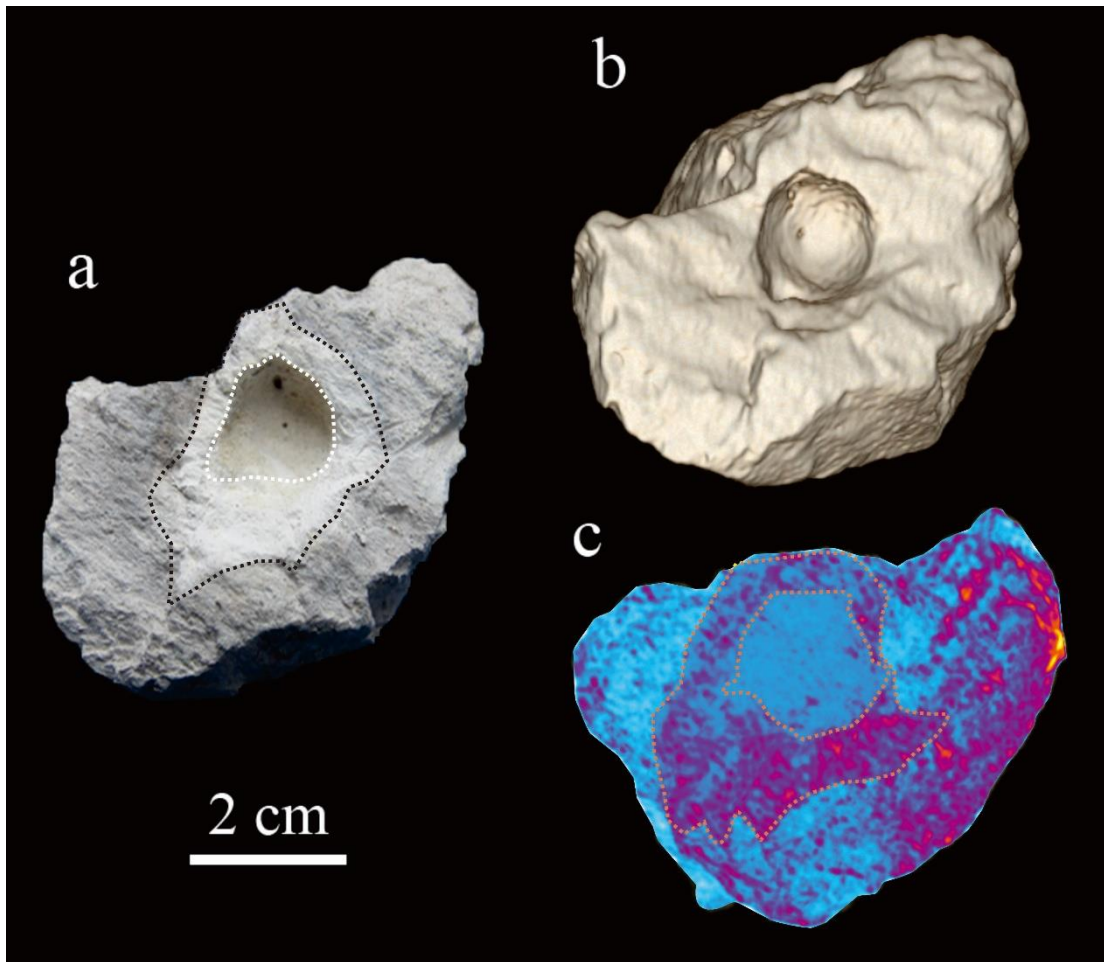
Figure 4: (a) A carbonate rock sample shows the enhanced of brightness associated with a burrow structure. (b) 3D reconstruction of the sample by CT shows the morphology of the sample. (c) 3D reconstruction of the sample by CT shows that the enhanced density is visible around the burrow, which is consistent with the enhanced brightness around the burrow as shown in Fig. 4 a.
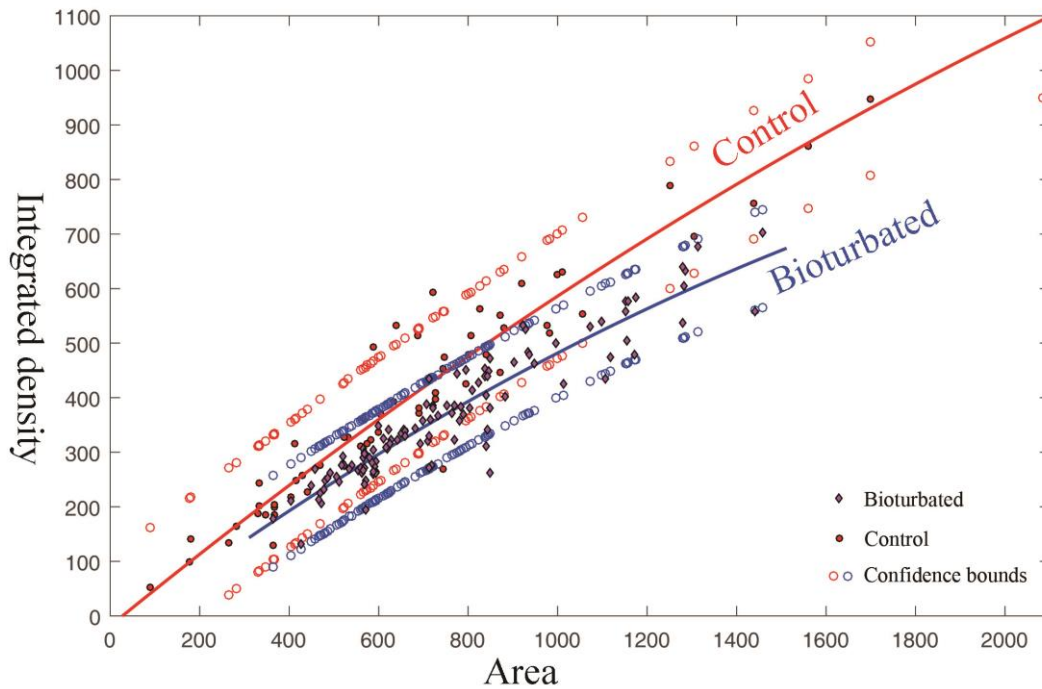
Figure 5: Statistical analysis of integrated density extracted from selected area around burrow and parallele undisturbed area shows different density around the burrows. Both images were inverted so that a larger integrated density means a darker color in the original CT image. The total number of analyzed burrows is 113. Although 95% confidence bounds are half overlain, the statistical significance indicated by the change in density can be shown from the curves. The goodness of fit is shown by $R^2_{bioturbate}=0.9312$ and $R^2_{control}=0.8802$.
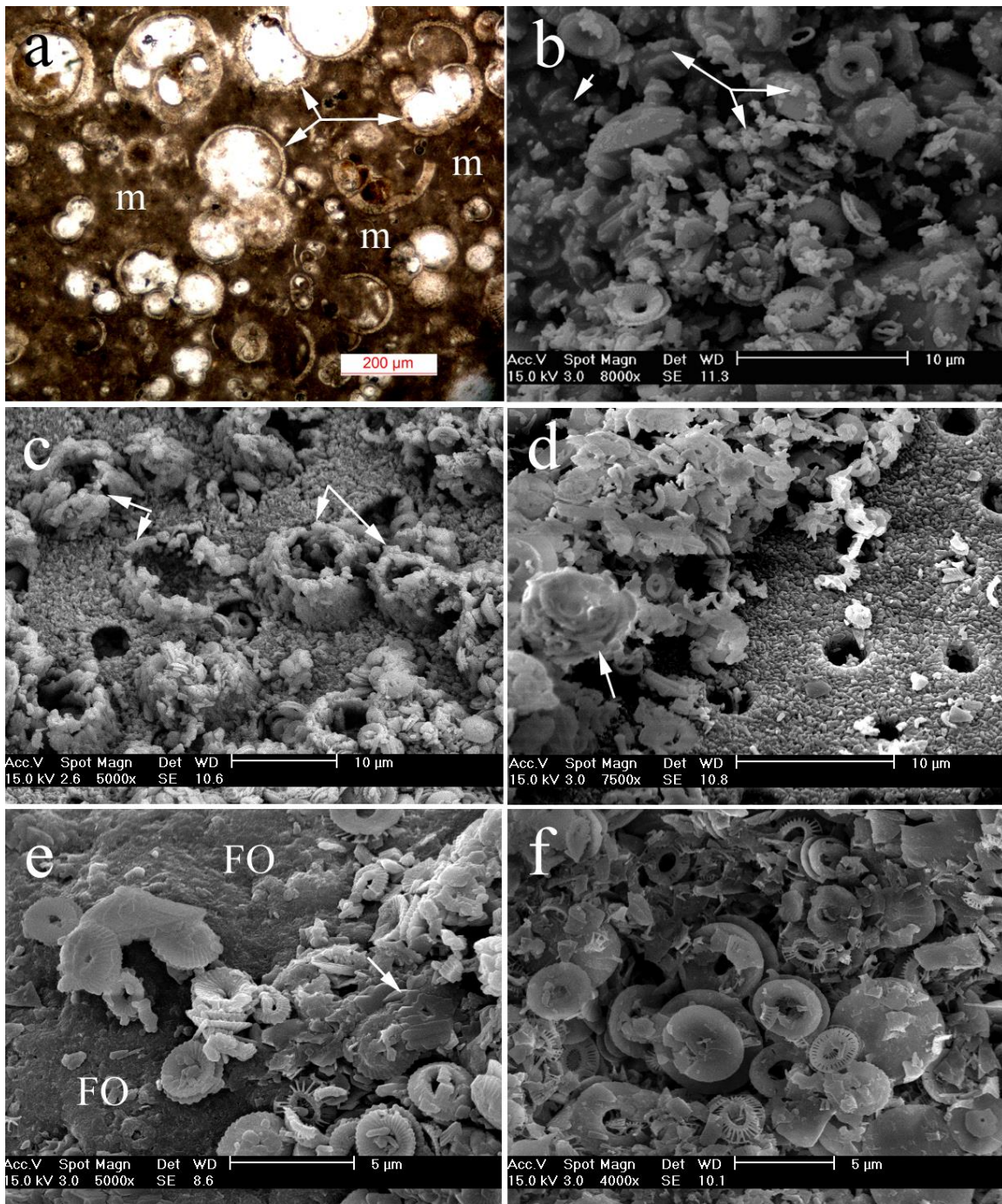
Figure 6: (a) Photomicrograph of thin sections of carbonate rocks shows a relatively high test (arrows) to matrix (m) ratio. (b) Scanning electron micrograph reveals abundant micritic carbonate particles (arrows) with many plates of coccoliths in the interior of carbonate rocks. (c) Scanning electron micrograph shows overgrowths of calcites on the foraminifera in the interior of carbonate rocks. (d) Scanning electron micrograph shows dissolution of coccoliths in the interior of carbonate rocks. (e) Scanning

electron micrograph shows the surface of carbonate rock covered by thin Mn- and Fe-oxide precipitates (FO). Arrow points out the dissolution ofcoccoliths. (f) Scanning electron micrograph shows gray sediments that infill the burrow. The smooth surfaces of the coccoliths indicate that dissolution commonly occurs.
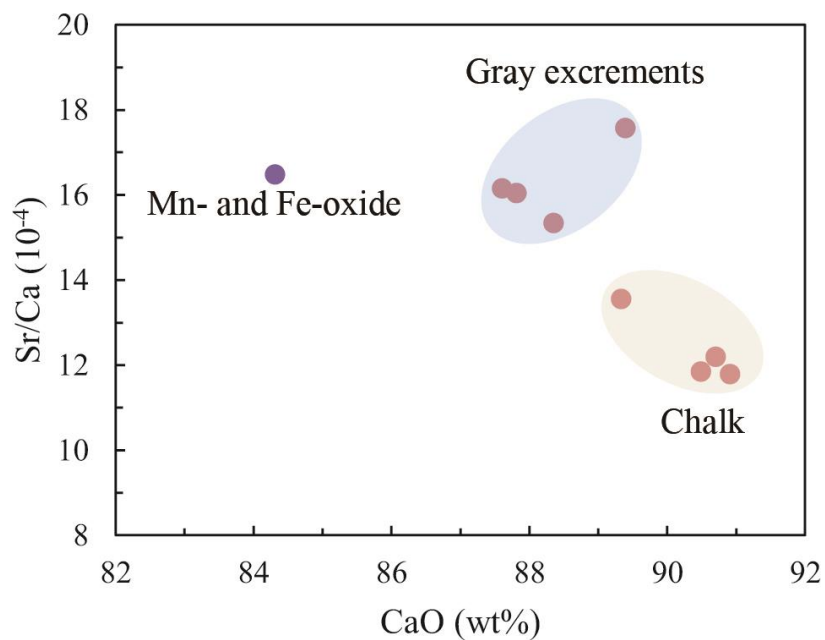
Figure 7: The lower Sr/Ca values in chalk compared to those observed in the gray excrements represents the lithification of different portions of carbonate.
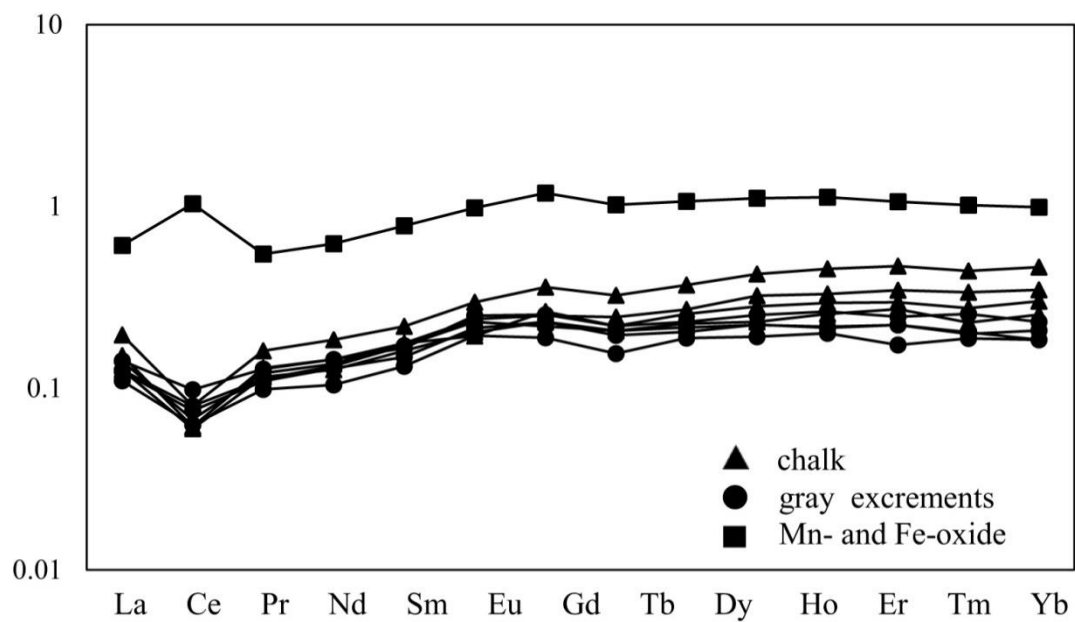
Figure 8: PAAS-normalized REE distribution patterns of selected samples from the SWIR.
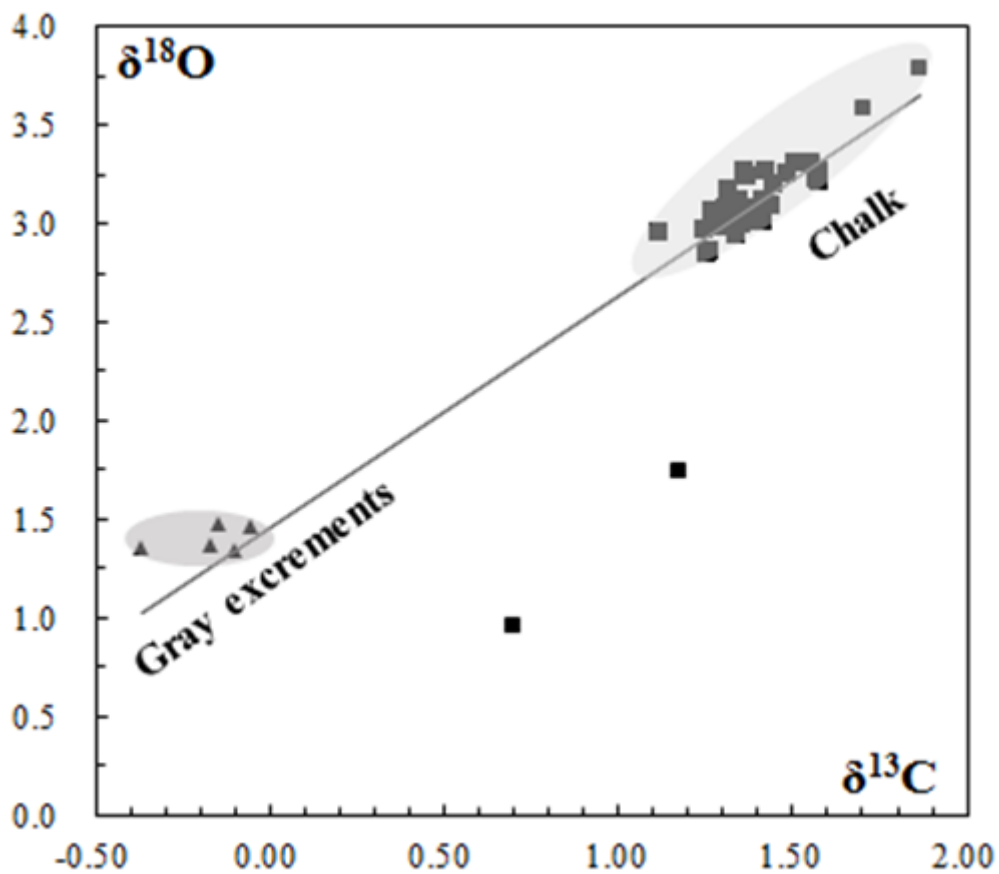
Figure 9: Oxygen and carbon isotopic composition of carbonate samples from the SWIR. Gray excrements contain lighter carbon and oxygen isotopic values than those in the chalk. The δ^{13}CPDB values of chalk and gray excrements are positively correlated with δ^{18}OPDB values (r=0.91).
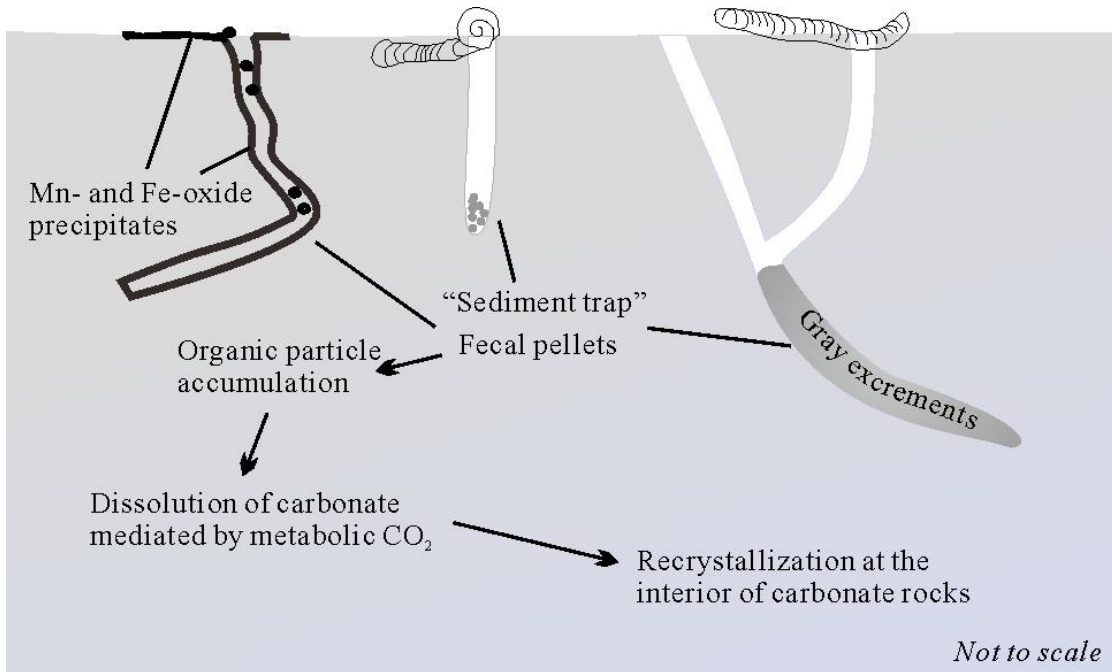
Figure 10: Schematic model for carbonate lithification influenced by bioturbation on the SWIR.

Sample NO.	δ¹³C PDB	δ¹⁸O PDB
1	1.36	3.04
2	1.28	2.99
3	1.30	3.09
4	-0.37	1.56
5	1.28	3.00
6	1.11	2.97

Table 1: Isotopic data for samples collected from Figure 3a. 1, 3 and 5 represent a higher density of influence by bioturbation compared to 2 and 6. 4 represents gray excrements infilling in the burrows.